

Solution of Team Benchmark Problem #9 Handling Velocity Effects with Velocity Dependent Green's Functions

ABSTRACT

A boundary element double layer formulation is applied to the problem of a coil moving down a conducting tube. The Green's function for the problem is nonsymmetric having a different value in front of the coil from that behind it. Results of the predicted B fields for $v=10$ and $v=100$ m/s are compared to the analytical solution of a coil traveling axially down the center of a conducting tube. Good agreement with the analytic solution is achieved for the field computations.

Integrated Engineering Software - Website Links

[Home](#)[Products](#)[Support](#)[Technical Papers](#)

"Page Down" or use scroll bars to read the article

SOLUTION OF TEAM BENCHMARK PROBLEM #9

Handling Velocity Effects with Velocity Dependent Green's Functions

Dalian Zheng
Integrated Engineering Software
#46 Border Place
Winnipeg, Canada R3H 0x4

Kent R Davey
School of Electrical Engineering
Georgia Institute of Technology
Atlanta, GA 30332-0250

Abstract

A boundary element double layer formulation is applied to the problem of a coil moving down a conducting tube. The Green's function for the problem is nonsymmetric having a different value in front of the coil from that behind it. Results of the predicted B fields for $v=10$ m/s and $v=100$ m/s are compared to the analytical solution of a coil traveling axially down the center of a conducting tube. Good agreement with the analytic solution is achieved for the field computations.

BOUNDARY ELEMENT THEORY

The problem to be analyzed is shown in Figure 1. The coil is excited at 50 Hz and is traveling down the pipe at velocity V . We analyze the problem with $V=0$ m/s and 10 m/s. The boundary element approach (BEM) employed asks what fictitious free surface currents K_f could be placed on the skin of this pipe to account for the magnetization of the iron and the eddy currents. Actually 2 sets of surface currents are employed. A skin of currents just inside the pipe shell perimeter is used to represent the fields everywhere in the pipe. Another set of currents just outside the shell models the field in the air. The surface currents on the air side at r just less than 14 mm, dictate the field in the air region $0 < r < 14$ mm. The surface currents just outside the skin at $r=20$ mm, dictate the field for $r > 20$ m. Once the surface currents are known, the magnetic field is found simply from Biot-Savart's law.

For the eddy current problem without movement, the pertinent equations for H and E are

$$\nabla \times \vec{H} = \sigma \vec{E} + \vec{J}_s \quad (1)$$

$$\vec{E} = -j\omega \vec{A} - \nabla \Phi \quad (2)$$

Writing (1) in terms of the vector potential A yields

$$\nabla \times \nabla \times \vec{A} - k^2 \vec{A} = \mu \vec{J}_s + \mu \sigma \nabla \Phi \quad (3)$$

where $k^2 = j\omega\mu\sigma$,
and $\nabla \cdot \vec{A} = \mu\sigma\Phi$.

With the specified gauge of (3), the curl curl equation can be replaced by

$$\nabla^2 \vec{A} + k^2 \vec{A} = -\mu \vec{J}_s \quad (4)$$

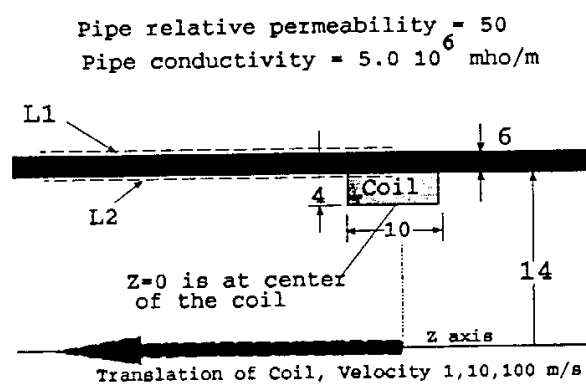


Figure 1 Coil traveling axially down a conducting pipe with velocity V .
All dimensions are in millimeters.

The integral solution for the vector potential due to a source current is [1-3],

$$\vec{A}(r) = \mu \oint G(r, r') K_f(r') dS' \quad (5)$$

where

$$G(r, r') = \frac{\mu}{2\pi} \int_0^\pi \frac{e^{jk_z |r-r'|}}{|r-r'|} dS'$$

Figure 2 helps to elucidate the approach. The fields in regions 1 and 2 are represented in terms of the surface currents and external impressed fields H_i and E_i as

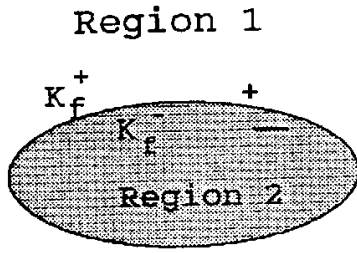


Figure 2 Two-region problem analyzed with BEM.

$$\vec{H}^+ = \vec{H}_1 + \vec{H}(K_f^+) \quad (6)$$

$$\vec{H}^- = \vec{H}(K_f^-) \quad (7)$$

$$\vec{E}^+ = \vec{E}_1 + \vec{E}(K_f^+) \quad (8)$$

$$\vec{E}^- = \vec{E}(K_f^-) = -j\omega A^- \quad (9)$$

It only remains to impose the boundary conditions on E and H which are

$$\hat{n} \times (\vec{E}_2^+ - \vec{E}_1^-) = -\hat{n} \times \vec{E}_1 \quad (10)$$

$$\hat{n} \times (\vec{H}_2^+ - \vec{H}_1^-) = -\hat{n} \times \vec{H}_1 \quad (11)$$

Here \hat{n} is the outward normal to region 1. Note that the condition $\hat{n} \cdot \vec{B} = 0$ is automatically insured by the use of the equivalent currents to directly compute B. The reader should note that enforcing continuity of tangential E also assures continuity of normal B. Employing these boundary conditions yields the governing equations

$$j\omega [\mu_2 \oint_{s'} G(k_2, r, r') K_f^+(r') dS' - \mu_1 \oint_{s'} G(k_1, r, r') K_f^-(r') dS'] = -E_1^t = 0. \quad (12)$$

$$\frac{1}{2} (K_f^+(r) - K_f^-(r)) - \oint_{s'} K_f^+(r') \frac{\partial}{\partial n'} G(k_2, r, r') dS' + \oint_{s'} K_f^-(r') \frac{\partial}{\partial n'} G(k_1, r, r') dS' = -\hat{n} \times \vec{H}_1 \quad (13)$$

VELOCITY EFFECTS

Velocity effects are incorporated by recalling that $\vec{J} = \sigma (\vec{E} + \vec{v} \times \vec{B})$. Using $\vec{E} = -j\omega \vec{A}$, Ampere's law becomes

$$\nabla^2 A_\phi - \mu \sigma \left(j\omega A_\phi + v \frac{\partial A_\phi}{\partial z} \right) = -\mu J_\phi^s \quad (14)$$

where J_ϕ^s represented the ϕ directed source current density. To get the Green's function, it is necessary to solve

$$\nabla^2 G(r, r') - \mu \sigma \left(j\omega G(r, r') + v \frac{\partial G(r, r')}{\partial z} \right) = -\mu \delta(\vec{r} - \vec{r}') \quad (15)$$

To find G, let $G(r, r') = e^{-\frac{\mu \sigma v z}{2}} g(r, r')$ and substitute this into (15) to give

$$(\nabla^2 + \gamma^2) g(r, r') = -\mu_0 e^{-\frac{\mu \sigma v z}{2}} \delta(\vec{r} - \vec{r}') \quad (16)$$

$$\text{where } \gamma^2 = -\left\{ j\omega \mu \sigma + \left(\frac{\mu \sigma v}{2} \right)^2 \right\}.$$

The solution of (16) yields the result

$$G(r, r') = \frac{\mu_0}{4\pi R} e^{-\gamma R} e^{-\frac{\mu \sigma v (z - z')}{2}} \quad (17)$$

where $R = |\vec{r} - \vec{r}'|$.

This is the Green's function that must be used in (12) and (13).

RESULTS

Radial Field Nonmagnetic Pipe

plotted along line L1 ($r=20.3$)

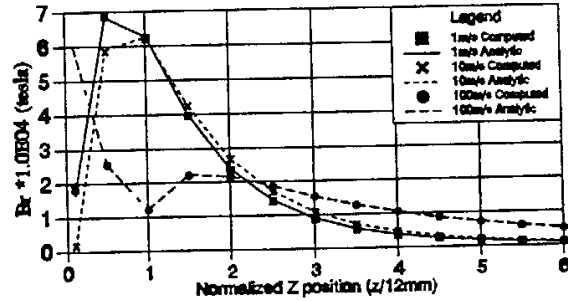


Figure 3 Radial field for the non-magnetic pipe on line L1 ($r=20.3$ mm).

Unknown surface currents were placed on either side of all air conductor interfaces. Linear basis functions were employed for the interfacial dependence of these fictitious surface currents. The problem used 816 elements with approximately 1632 unknowns and was solved on an HP 710 workstation in 15 minutes. The problem is worked with the pipe being nonmagnetic and magnetic ($\mu_r=50$), both cases have conductivity $\sigma = 5 \times 10^6 \text{ U/m}$. Shown in Figure 3 is the

magnitude of the radial field for the nonmagnetic pipe on the outer line L1. All field values have been multiplied by 10^4 .

The axial field measurements for the same case and velocity variation are shown in Figure 4.

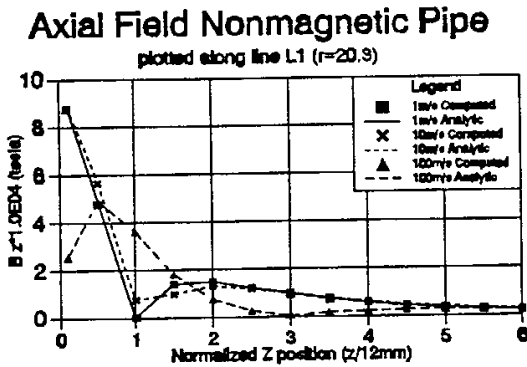


Figure 4 Axial field along line L1 for various velocity settings.

As witnessed by the plots, the field predictions are quite good. The ferromagnetic pipe is more problematic due to the size of the exponential argument. The prediction of the radial field along the same line L1 is shown in Figure 5.

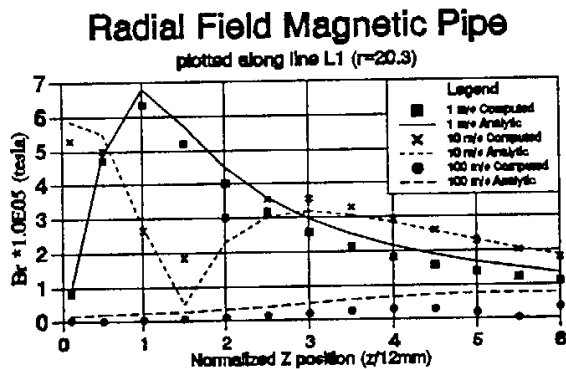


Figure 5 Radial field prediction along line L1 for the magnetic pipe.

The corresponding axial field for the ferromagnetic field is shown in Figure 6.

By way of completeness, Figure 7 shows the field predictions on the inner line L2. On first glance it would appear that field predictions are excellent. Actually the large argument index $\mu\sigma v z$ is beginning to become a problem numerically.

This is more clearly demonstrated in the plot of the axial field for the same line shown in Figure 8. The high speed 100 m/s case is beginning to diverge from the analytic solution quite a bit. The modeled tube length was 340 mm. At

Axial Field Magnetic Pipe

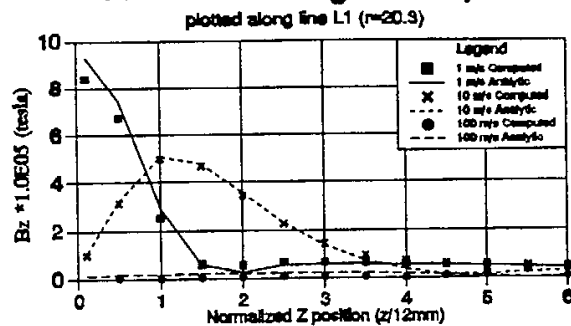


Figure 6 Magnitude of the axial field for the ferromagnetic field along line L1.

this length the argument $\mu\sigma v z$ is becoming quite small. The entries in the governing matrix in this region are becoming more similar for negative z , i.e., almost zero. Accurate predictions in these circumstances will undoubtedly require double precision.

Radial Field Magnetic Pipe

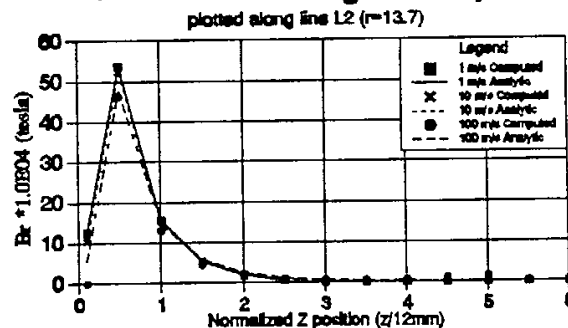


Figure 7 Radial B field on line L2 for the ferromagnetic pipe.

The voltage induced in a pickup coil having the same dimensions as the exciting coil was also computed. The coil was located at the same radius and displaced 112 mm ahead of the exciting coil. Table I shows the predicted voltages computed by integrating the flux linking the coil and multiplying by $j\omega$. The predicted voltages do not agree with the analytic solution, either with the coil placed ahead or behind the exciting coil. The agreement of the two solutions for the raw B field makes this team suspect some error with the analytic solution. Table II shows the same voltage computations for the ferromagnetic pipe case.

Axial Field Magnetic Pipe

plotted along line L2 ($r=13.7$)

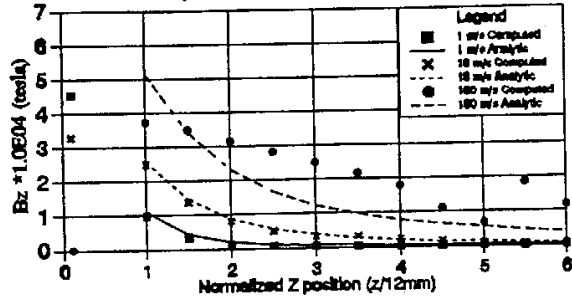


Figure 8 Axial field on the lower segment L2 for the ferromagnetic pipe.

voltages presented is correct, and that some error has occurred in the analytic prediction of the same.

ACKNOWLEDGEMENTS

The BEM package used for these calculations was built upon a boundary element called Oersted from Integrated Engineering Software.

REFERENCES

- [1] Smythe, *Static and Dynamic Electricity*, McGraw Hill, 1965, p 290.
- [2] M. Burnet-Fauchez and R. Michaux, "Boundary Element Calculation of 2D magnetic fields with eddy currents", *Modeler Conf. La Grande Motte*, Oct. 1984, Pluralis Ed. Paris, pp 97-109.
- [3]. M. Burnet-Fauchez, "Calculation of eddy currents in moving conductors using boundary element methods", *Proc. COMPUMAG*, Colorado State, Fort Collins, June 3-6, 1985.

Table I Induced voltages for the Non-ferromagnetic Tube

Velocity m/sec	Coil Ahead		Coil Behind		Analytic Solution	
	Mag*10 ⁴ Phase		Mag*10 ⁴ Phase		Mag*10 ⁴ Phase	
0	6.38	0	6.38		0.69	
1	6.438	90	9.59	77.8		
10	5.385	78.3	7.77	76.6	0.842	-92
100	1.952	81.9	6.72	74.9	7.23	-92

Table II Induced voltages for the Ferromagnetic Tube

Velocity m/sec	Coil Ahead		Coil Behind		Analytic Solution	
	Mag*10 ⁴ Phase		Mag*10 ⁴ Phase		Mag*10 ⁴ Phase	
0	1.211	-22.2	1.211	-22.2	0.254	-112
1	1.127	-11.6	2.66	-28.9		
10	0.593	-21.4	1.3	-22.9	0.475	-111
100	5.4E-4	33.8	72.6	69.6	1.96	-93

CONCLUSIONS

Boundary element codes are quite suited to some problems involving motion induced eddy currents. For any problem involving translation, the Green's function discussed is suitable. With rotation, however, the Green's function must have radial dependence. These authors are not aware of a suitable Green's function to handle rotational induced eddy currents. Because of the good agreement of the fields with the analytic solution, these authors feel the solution for the